Evolution of Microstructural Banding during the Manufacturing Process of Dual Phase Steels

Francisca G. Caballero, Andrea García-Junceda*, Carlos Capdevila and Carlos García de Andrés.

Solid-Solid Phase Transformations Group (MATERALIA), Centro Nacional de Investigaciones Metalúrgicas (CENIM), Consejo Superior de Investigaciones Científicas (CSIC), Avda. Gregorio del Amo, 8, 28040 Madrid, Spain

Synopsis

The segregation of manganese during solidification from casting is responsible for banding problems of dual phase steels. Microstructural banding lasts during all the manufacture process, producing the deterioration of the material, so the final ductility and impact toughness of the sheets are decreased due to the high level of anisotropy. To avoid or reduce the problem of microstructural banding, it is proposed to modify the hot rolling parameters so the

* Graduate Student, Complutense University of Madrid

formation of ferrite-pearlite microstructures is avoided and thus the presence of banding. The study of the microstructural evolution during the whole manufacturing process reveals that the increase of the cooling rate during the hot rolling leads to a significant decrease of martensite banding in the microstructure of dual phase steels for sheets used in the automotive industry.

Keywords: dual-phase steel, intercritical annealing, banding

Abridged title: Microstructural Banding in Dual Phase Steels

1. Introduction

Dual phase steels were developed to provide high strength formable alloys for the automobile industry. They consist of a mixture of martensite and ferrite. The strains associated with the formation of martensite introduce free dislocations in the adjacent ferrite, thereby eliminating the sharp yield points and avoiding stretcher strains. The mixture of hard martensite and soft ferrite also gives a higher average strength without sacrificing formability (uniform ductility)[1-7].

Low-carbon compositions mainly strengthened with manganese and silicon are used to produce dual phase steels with high formability. Other alloy content of the steel has to be carefully selected to generate a level of hardenability that will enable the martensite transformation to occur directly by carefully controlled hot rolling[8]. For thinner gauges, dual phase steels can also be produced after cold rolling by intercritical annealing in the ferrite/austenite field, followed by rapid cooling.

It is well known that in hot rolled low alloy steels, pearlite and ferrite are, as a rule, arranged in layers. In longitudinal section, this arrangement is visible as a banded structure[9,10]. Hot rolled bands remains inalterable after cold rolled and continuous annealing of dual phase steels, since during the intercritical heat treatment austenite formation takes place only in the carbon-rich regions featuring pearlite, while the low-carbon regions remain ferritic[11]. When rapid cooling, martensite will then form in the regions previously occupied

by pearlite. The banded appearance of the microstructure affects mainly the ductility and the impact energy of the steel, while other mechanical properties are not significantly altered[12,13]. In addition, some properties can be impaired such as machinability, hydrogen-induced cracking, or cracking in the heat-affected zone during welding[14-16].

Microstructural banding is due to the segregation of substitutional alloying elements during dendritic solidification. Several investigations have shown manganese to be the alloying element most responsible for the development of microstructural banding in low alloy steels[10-12]. Moreover, austenitising temperature, austenite grain size, and cooling rate influence the severity of microstructural banding[17]. Thompson and Howell[18] investigated banding in 0.15 wt-%C, 1.40 wt-%Mn steel and concluded that increasing the cooling rate from the austenitic condition reduces the intensity of banding because it reduces the Ar_3 temperature differences of the segregated bands. However, it is not clear if banding eliminated by fast cooling during hot rolling of dual phase steels could appear in subsequent stages of the manufacturing process such as cold rolling and intercritical annealing. In the present work, the cooling rate and coiling temperature during hot rolling simulation of a dual phase steel has been modified so the formation of ferrite-pearlite microstructures is avoided and thus the presence of banding. The study of the microstructural evolution during the whole manufacturing process has revealed the possibilities of permanently eliminate microstructural banding in cold rolled dual phase steels.

2. Experimental Procedure

The dual phase steel investigated contained, in wt-%, 0.15C, 1.9Mn, 0.2Si, 0.2Cr, 0.03Al, and 0.015P. This steel was elaborated using a 60kg vacuum induction furnace under inert atmosphere. Semi rolled slabs 30 mm thick were soaked at 1200°C for 45 min. and hot rolled to about 3mm in several passes finishing at 900ºC. Two different cooling rates (*CR*, 7 and 60 ºC/s) and two different coiling temperatures (*CT*, 500 and 650ºC) were tested in the pilot hot-rolling mill. After removing scale, the hot-rolled samples were cold rolled by reduction in thickness of 68%. After cold rolling, 12 mm x 2 mm x 0.9 mm samples were machined parallel to the rolling direction and used for the simulation of the intercritical annealing. For this purpose, the heating and cooling devices of a high-resolution dilatometer were used[19].

Hot and cold rolled specimens, parallel and transverse to the rolling direction, were ground and polished using standardised techniques for metallographic examination. A 2 pct Nital etching solution was used to reveal the microstructure by optical and electron microscopy. The volume fraction of pearlite, $V_{P,}$ in microstructures consisting of ferrite and pearlite was estimated by a systematic manual point counting procedure on optical micrographs[20].

To reveal more in detail the microstructure of the steel, scanning electron microscopy (SEM) was carried out on a JEOL JSM-6500F Field Emission Scanning Electron Microscope operating at 7 kV. Thus, it was possible to characterise the lamellar microstructure of pearlite. Two parameters, the mean true interlamellar spacing, σ_0, and the area per unit volume of the pearlite colonies interface, S_v^{PP}, are measured to fully characterise the lamellar microstructures. The values of σ_0 were derived from electron micrographs according to Underwood´s intersection procedure[20]. Moreover, the values of S_v^{PP} are obtained by counting the number of intersections of the pearlite colony boundaries with the circular test grid as reported by Roosz *et al*[21].

Annealing was carried out within the intercritical temperature range, which was determined experimentally by monitoring the fractional change in dilatation with temperature in cold rolled samples heated up to 1000 ºC at a rate of 5 ºC/s. Table 1 lists the Ac_1 and Ac_3 temperatures of the different samples tested. Cold rolled specimens were intercritical annealed at three different soaking temperatures (750, 800 and 850 ºC) for different times (1, 20 and 100 s) before gas quenching. The heating rate selected for the intercritical annealing experiments was 5 ºC/s. Austenite, which is formed during intercritical annealing, transforms to martensite during quenching. Thus, the progress of austenitisation is determined throughout the evolution of the volume fraction of martensite. In this sense, annealed specimens were polished in the usual way for metallographic examination. LePera's reagent[22] was used to reveal martensite formed during

quenching. The quantitative measurement of martensite volume fraction was carried out by point-counting method[20] in longitudinal sections. Likewise, a reagent based on saturated aqueous picric acid plus a wetting agent was used to reveal the austenite grain boundaries on annealed samples[23]. The austenite grain size (*AGS*) was determined on optical micrographs with the help of an image analyser and results were analysed in terms of mean values of the equivalent circle diameter.

The Standard Practice ASTM E 1268-99 for "Assessing the Degree of Banding or Orientation of Microstructures" gives the following definition of banded microstructure based on its morphological appearance: 'separation, of one or more phases or constituents in a two-phase or multiphase microstructure, into distinct layers parallel to the deformation axis due to elongation of microsegregation'[24]. The practice proposes the characterisation of the degree of banding in the microstructure by the anisotropy index, *AI*, and the mean edge-to-edge spacing of the bands, λ, which rely on simple stereological methods. The anisotropy *AI* is estimated from the following equation,

$$AI = \overline{N}_{L\perp} / \overline{N}_{L\square} \qquad (1)$$

where $\overline{N}_{L\perp}$ is the mean number of feature interceptions with test lines perpendicular to the deformation direction per unit length of the test lines, and $\overline{N}_{L\parallel}$ is the mean number of feature interceptions with test lines parallel to the deformation direction per unit length of the test lines. For a randomly oriented, non-banded microstructure, AI has a

value of one. As the degree of orientation or banding increases, the anisotropy index increases.

The mean free path spacing, λ, is determined as follows,

$$\lambda = (1 - V_V) / \bar{N}_{L\perp} \quad (2)$$

where V_V is the volume fraction of the banded or the oriented phase.

3. Results and Discussion

3.1. Microstructure of hot and cold rolled samples

Optical and scanning electron micrographs of hot rolled samples are shown in Fig. 1. Samples cooled at 7 ºC/s after finishing (S1 and S3) exhibit a ferrite and pearlite microstructure. The volume fraction of pearlite in those samples depends on the coiling temperature applied. Thus, sample S1 coiled at 500 ºC is mainly formed of ferrite and less than 5% randomly dispersed pearlite is present in the microstructure. Whereas, sample S3 coiled at higher temperature (650 ºC) presents a significant amount of pearlite in bands. On the other hand, hot rolled samples more rapidly cooled after finishing (S2 and S4) consist mainly of bainite and martensite. Micrographs suggest that microstructural banding can be suppressed increasing the cooling rate and/or decreasing the coiling temperature during hot rolling process. This

confirms that avoiding the formation of a significant amount of pearlite during cooling, it is possible to prevent the presence of bands on hot rolled microstructures.

As mentioned above, the underlying cause of microstructural banding is compositional segregation mainly in the form of alternating rich and lean manganese layers. However, as Fig. 1(a), 1(c) and 1(g) demonstrate, microstructural banding does not always appear in steel with compositional gradient. At high enough cooling rates and/or low enough coiling temperatures to form bainite and/or martensite in both rich and lean manganese bands, the underlying pattern of segregation can be hidden behind an uniform bainitic or martensitic microstructure. By contrast, at cooling rates slower than the critical velocity to form bainite in both bands, and/or at coiling temperatures too high to form bainite in both bands, microstructural banding appears to be due to the effects of alloy chemistry on the nucleation and growth of ferrite and pearlite (See Fig. 1(e)).

The formation of pearlite bands is associated to the redistribution of carbon between rich and lean manganese bands. Ferrite allotriomorphs start to nucleate in lean manganese regions with high Ar_3 temperature, which cause the carbon to redistribute. The carbon is piled up in rich manganese regions with a low Ar_3 temperature. This increase in carbon content in the adjacent austenite will lower the local Ar_3 temperature even further. Eventually, the composition in these regions becomes the level required for pearlite nucleation and pearlite will form if the temperature is below the Ar_1 temperature. The growth of

pearlite layer can be only limited by decreasing carbon diffusion with decreasing transformation temperatures.

Fig. 2 shows the 68% cold rolled microstructure of the samples tested. The ferrite grains and the pearlite colonies are elongated, and deformation bands are present in the ferrite. The amount of pearlite in sample S3 exhibiting a banded ferrite and pearlite microstructure remains invariable after cold rolling (See results on V_P, in Table 2). By contrast to Rocha *et al*. results[25], islands of MA constituent were not observed in this cold rolled sample. Likewise, pearlite colonies present a lamellar structure as scanning electron micrographs revealed (See an example in Fig. 2(f). Cementite lamellae do not seem to be evidently fragmented and irregularly spaced as Yang *et al*. reported[26]. The determination of the morphological parameters of pearlite before and after cold rolling, listed in Table 2, demonstrated that deformed pearlite exhibits finer interlamellar spacing, σ_0, and higher area per unit volume of colonies interface, S_v^{PP} i.e. smaller pearlite colonies. This refinement is related to the approach of neighbouring cementite lamellae due to cold work, more noticeable in transverse section.

Regarding microstructural banding, only those hot rolled samples with bands were found to have banding problems after cold rolling. Quantitative characterisation of banding revealed that cold rolling significantly increases the anisotropy index, *AI*, and reduces the mean free path spacing, λ (See results in Table 2). *AI* values measured in longitudinal cold rolled samples were found to be much higher that those measured in transversal samples. Such difference was not

detected in the corresponding hot rolled sample. On the other hand, λ value gives us an idea of the distance between bands. In this sense, it is not surprising that λ value is reduced during cold rolling.

3.2. Microstructure of annealed samples

Fig. 3 shows microscopic evidences of how austenite formation occurs in cold rolled sample S3 (*CR*=7 ºC/s, *CT*=650 ºC) throughout optical micrographs from intercritical annealing specimens at different temperatures and times. LePera's reagent reveals pearlite and ferrite as darker phases in the microstructure, whereas martensite formed during quenching appears as lighter regions in the micrographs. When a specimen contains more than 60% martensite, contrast between ferrite and martensite begins to degrade[22]. In that case, ferrite appears as the lightest grey regions (See micrographs in Fig. 3(e), 3(f) and 3(g)). Microstructure in Fig. 3(a) is formed mainly of ferrite, pearlite and some grains of martensite. At this quench-out time, the pearlite-to-austenite transformation has already started. Once pearlite dissolution has finished annealed microstructure consists of a mixture of ferrite and martensite (Fig. 3(b) and 3(c)). Increasing the soaking temperature from 750 ºC to 800 ºC resulted in lower amounts of ferrite in the microstructure (Fig. 3(d), 3(e) and (3f)). This is due to the larger amount of austenite formed at higher temperatures, which transforms into martensite on quenching. At 850 ºC, when the intercritical soaking

is reached, a few ferrite grains remain un-transformed (Fig. 3(g)). But, it takes less than 20 s to completed the transformation to austenite, as a consequence a fully martensitic microstructure is formed on quenching (See Fig. 3(h) and 3(i)).

At 750 ºC and 1 s of soaking time, austenitisation process has already started for all the initial microstructures. Fig. 4 shows electron micrographs corresponding to the beginning of the transformation in annealed samples. It is clear from those micrographs that in samples consisting on ferrite and pearlite (samples S1 and S3), the nucleation of austenite takes place inside pearlite preferentially at the points of intersection of cementite with the edges of the pearlite colony (See Fig. 4(c). Likewise, in samples mainly formed by bainite (samples S2 and S4), austenite nucleates at the interface between the plates of ferrite in the sheaves of bainite (Fig. 4(b) and 4(d)). Moreover, carbides at grain boundaries and inside ferritic grains are an important nucleation site for austenite in cold rolled samples.

Ferrite recrystallisation was completed during heating in all the tested samples (See Fig. 4). In all the cases when the intercritical annealing stage is reached, the ferrite grains are fully recrystallised. This is in agreement with earlier reported data for different chemical compositions[25,27]. On the other hand, Fig. 4(c) suggests that pearlite spherodised before austenite formation. Spherodisation of the deformed pearlite occurs concurrently with ferrite recrystallisation during annealing of the cold rolled samples[26].

Even if ferrite recrystallisation did not take place during heating, the mechanism of austenite formation in the cold rolled steel would be controlled by the same mechanism as in the un-deformed microstructures, namely, carbon diffusion in austenite as concluded by Speich *et al*[26,27]. Thus, the volume fraction of austenite and its coarseness increase with increasing soaking temperature and time. This is in agreement with experimental results in Fig. 5. However, this figure suggests that the initial microstructure slightly affect the kinetics of austenite formation and its coarsening. Thus, austenitisation process is completed during heating at 850 ºC in samples S1 and S2, whereas about 10 % of ferrite is still un-transformed in samples S3 and S4. These kinetics results are also in accordance with dilatometric data listed in Table 1. Likewise, experimental results on the austenite grain coarsening during austenite formation (Fig. 5(b)) reveal that samples coiled at 500ºC in the hot rolling stage (samples S1 and S2) exhibit slightly finer austenite grains than those coiled at 650ºC (samples S3 and S4). It seems that samples S3 and S4, both coiled at 650 ºC, exhibit more sluggish formation of austenite associated with a higher amount of dispersed carbides in the cold rolled microstructure (See Fig. 4(c) and 4(d) of both samples. This is consistent with manganese partitioning as observed by other investigators[28,29].

It is clear from Fig. 3 that cold rolled bands do not vanish during intercritical annealing, since austenite formation starts in the carbon-rich regions featuring pearlite. Thus, martensite bands will form during quenching in the regions previously occupied by pearlite. However, it is not clear if martensite bands will reappear during intercritical

annealing once banding was eliminated by fast cooling during hot rolling. Fig. 6 shows the evolution of the anisotropy index, *AI*, and the mean edge-to-edge spacing of the bands, λ, during intercritical annealing. Both parameters characterise the degree of martensite banding on longitudinal sections. Those samples with a non-banded microstructure present a AI value of one. That is the case of samples annealed at 850ºC consisted mainly of martensite whose AI values have not been included here.

Only samples S1 and S3, both slowly cooled during rolling, present microstructural banding at 750ºC, more severe in sample S3 initially consisted of ferrite-pearlite bands. Martensite bands did not appear in samples S2 and S4, both rapidly cooled during rolling, at the same soaking temperature. However, all the samples that originally did not present banding (samples S1, S2 and S4), exhibit a banded martensitic microstructure after an intercritical annealing at 800 ºC (See micrographs in Fig. 7). At this temperature the *AI* value increases as the transformation proceeds with time, approaching an *AI* value close to that measured on the initial hot rolled banded ferrite and pearlite microstructure (about 2). This is not surprising since hot rolled pearlite bands roughly resemble original manganese segregation. On the other hand, λ values decrease as transformation proceeds (Fig. 6(c)) since bands of austenite get closer.

It seems that decreasing the coiling temperature during hot rolling is not an efficient practice to suppress microstructural banding, although an attenuation of the problem was detected after intercritical annealing

at 750 ºC. By contrast, rapid cooling during hot rolling has proved to be successful avoiding bands formation during intercritical annealing at the same temperature.

In general, samples rapidly cooled during hot rolling stage (samples S2 and S4), consisting mainly of bainite and martensite, exhibit the lowest degree of banding after intercritical annealing. It is also remarkable that, annealed samples at 750 ºC for 100 s present much less severe banding problem that those annealed at 800 ºC for 1 s, although the volume fraction of austenite formed in both cases is quite similar (around 30%) as Fig. 7 illustrates. A more homogeneous nucleation site distribution of smaller austenite grains at the lowest soaking temperature, would explain the less severity of banding observed at 750 ºC for 100 s in comparison to 800 ºC for 1 s. Therefore, increasing the cooling rate during hot rolling, and using low intercritical annealing temperatures and longer soaking time is possible to permanently eliminate microstructural banding in cold rolled dual phase steels.

4. Conclusions

The study of the microstructural evolution during the whole manufacturing process of a dual phase steel has showed that banding eliminated by fast cooling during hot rolling will appear after intercritical annealing at 800 ºC. In that case, the degree of banding

will increase as the transformation proceeds resembling the original chemical segregation.

However, it has been found that increasing the cooling rate during hot rolling, and using low intercritical annealing temperatures (750 ºC) and longer soaking time (100 s) is possible to permanently eliminate microstructural banding in cold rolled dual phase steels.

5. Acknowledgements

The authors express their gratitude for the financial support from the European Coal and Steel Community (ECSC-7210-PR-349). Andrea García-Junceda would like to express her gratitude to the Spanish Ministerio de Educación y Ciencia for the financial support in the form of a PhD Research Grant (FPU Program). The authors are extremely grateful to Dr. T. Iung from Arcelor Research – Metz (France) for fruitful discussions.

6. References

1) K Araki, Y Takada and K Nakaoka: Trans. Iron Steel Inst. Jpn. **17** (1977) 710-717.
2) W.S. Owen: Met. Technol. **7** (1980) 1-13.
3) CI Garcia and AJ Deardo: JOM. **32** (1980) 24-25.
4) SS Hansen and RR Pradhan: JOM. **32** (1980) 30-30.
5) NK Balliger and T Gladman: Met. Sci. **15** (1981) 95-108.
6) MS Rashid: Annual Review of Mater. Sci. **11** (1981) 245-266.
7) JD Embury and JL Duncan: JOM. **34** (1982) 24-29.
8) DT Llewellyn and DJ Hillis: Ironmaking & Steelmaking. **23** (1996) 471-478.
9) G Krauss: Metall. Mater. Trans. B. **34** (2003) 781-792.
10) V Faccenda, M Falco and C Modena: Metall. Ital. **65** (1973) 133-140.
11) R Grossterlinden, R Kawalla U Lotter and H Pircher: Steel Res. **63** (1992) 331-336.
12) R. A. Grange: Metall. Trans. **2** (1971) 417-426.
13) A. Sakir Bor: ISIJ Int. **31** (1991) 1445-1446.
14) GR Wilms and RL Aghan: Met. Technol. **8** (1981) 108-112.

15) K.K. Chawla, J.M. Rigsbee and JB Woodhouse: J. Mater. Sci. **21** (1986) 3777-3782.

16) AJ Gouch and H. Muir: Metals Forum. **3** (1980) 143-150.

17) T. F. Majka, D.K. Matlock and G. Krauss: Metall. Mater. Trans. A, **33A** (2002) 1627-1637.

18) SW Thompson and PR Howell: Mater. Sci. Technol. **8** (1992) 777-784.

19) C. García de Andrés, F.G. Caballero, C. Capdevila and L.F. Alvarez: Mater. Charact. **48** (2002) 101–111.

20) E.E. Underwood: *Quantitative Stereology*, (Addison-Wesley Publishing Co., Reading, MA, 1970) pp. 73-75.

21) A. Roósz, Z. Gácsi and E.G. Fuchs: Acta Metall. **31** (1983) 509-517.

22) F.S. LePera: Metallography. **12** (1979) 263-268.

23) C. García de Andrés, M.J. Bartolomé, C. Capdevila, D. San Martín, F.G. Caballero and V. López: Mater. Charact. **46** (2001) 389-398.

24) ASTM standard E 1268-99: *Annual Book of ATM Standard,* (ASTM, Philadelphia, PA, 1999) pp. 1-29.

25) R.O. Rocha, T.M.F. Melo, E.V. Pereloma and D.B. Santos: Mater. Sci. Eng. **39A** (2005) 296-304.

26) D.Z. Yang, E.L. Brown, D.K. Matlock and G. Krauss: Metall. Trans. A. **16A** (1985) 1385-1392.

27) G.R. Speich, V.A. Demarest and R.L. Miller: Metall. Trans. A. **12** (1981) 1419-1428.

28) CI Garcia and AJ DeArdo: Metall. Trans. A. **12** (1981) 521-530.

29) XL Cai, AJ Garratt-Reed and WS Owen: Metall. Trans. A. **16** (1985) 543-557.

Total number of letters and words used: 20645 letters, 3694 words.

List of Captions of Tables and Figures

Table 1 Hot rolled conditions and heating critical temperatures of cold rolled samples.

Table 2 Characterisation of banded ferrite-pearlite microstructures in hot and cold rolled samples. Sample S3: *CR*=7 ºC/s, *CT*=650 ºC.

Figure 1 Light optical micrographs and scanning electron micrographs of hot rolled specimens parallel to the rolling direction: (a)(b) Sample S1: *CR*=7 ºC/s, *CT*=500 ºC; (c)(d) Sample S2: *CR*=60 ºC/s, *CT*=500 ºC; (e)(f) Sample S3: *CR*=7 ºC/s, *CT*=650 ºC; (g)(h) Sample S4: *CR*=60 ºC/s, *CT*=650 ºC. B is bainite, M is martensite, F is ferrite and P is pearlite.

Figure 2 Light optical micrographs and scanning electron micrographs of 68% cold rolled specimens parallel to the rolling direction: (a)(b) Sample S1: *CR*=7 ºC/s, *CT*=500 ºC; (c)(d) Sample S2: *CR*=60 ºC/s, *CT*=500 ºC; (e)(f) Sample S3: *CR*=7 ºC/s, *CT*=650 ºC; and (g)(h) Sample S4: *CR*=60 ºC/s, *CT*=650 ºC.

Figure 3 Optical micrographs from intercritical annealed samples: (a) at 750 ºC for 1 s; (b) at 750 ºC for 20 s; (c) at 750 ºC for 100 s; (d) at 800 ºC for 1 s; (e) at 800 ºC for 20 s; (f) at 800 ºC for 100 s; (g) at 850 ºC for 1 s; (h) at 850 ºC for 20 s; (i) at 850 ºC for 100 s. Initial microstructure: cold rolled sample S3 (*CR*=7 ºC/s, *CT*=650 ºC). LePera reagent.

Figure 4 Scanning electron micrographs corresponding to the beginning of the austenitisation process in annealed samples at 750 ºC for 1 s. Initial microstructure: (a) sample S1 (*CR*=7 ºC/s, *CT*=500 ºC); (b) sample S2 (*CR*=60 ºC/s, *CT*=500 ºC); (c) sample S3 (*CR*=7 ºC/s, *CT*=650 ºC); and (d) sample S4 (*CR*=60 ºC/s, *CT*=650 ºC). 2 pct Nital etching solution.

Figure 5 Evolution of (a) austenite volume fraction and (b) austenite grain size during intercritical annealing. Sample S1 (*CR*=7 ºC/s, *CT*=500 ºC); Sample S2 (*CR*=60 ºC/s, *CT*=500 ºC); Sample S3 (*CR*=7 ºC/s, *CT*=650 ºC); and Sample S4 (*CR*=60 ºC/s, *CT*=650 ºC).

Figure 6 Evolution of microstructural banding during intercritical annealing: Anisotropy index (a) at 750 ºC and (b) at 800 ºC of soaking temperature; and (c) mean edge-to-edge spacing of the bands, λ. Sample S1 (*CR*=7 ºC/s, *CT*=500 ºC); Sample S2 (*CR*=60 ºC/s, *CT*=500 ºC); Sample S3 (*CR*=7 ºC/s, *C*T=650 ºC); and Sample S4 (*CR*=60 ºC/s, *CT*=650 ºC).

Figure 7 Evolution of microstructural banding during intercritical annealing in sample S4 (*CR*=60 ºC/s, *CT*=650 ºC): (a) 750 ºC, 20 s; (b) 750 ºC, 100 s; (c) 800 ºC, 1 s; and (d) 800 ºC, 20 s. LePera reagent.

Tables and Figures

Table 1 Hot rolled conditions and heating critical temperatures of cold rolled samples.

Sample	*CR*, ℃/s	*CT*, ℃	Ac_1, ℃	Ac_3, ℃
S1	7	500	734	846
S2	60	500	737	849
S3	7	650	734	856
S4	60	650	738	853

CR Cooling rate; *CT* Coiling temperature

Table 2 Characterisation of banded ferrite-pearlite microstructures in hot and cold rolled samples. Sample S3: *CR*=7 ºC/s, *CT*=650 ºC.

	V_P	σ_0 (μm)	$S_v^{PP} * 10^{-3}$ (μm^{-1})	*AI*	λ (μm)
Hot rolled sample					
Longitudinal	0.30 ± 0.02	0.19 ± 0.02	616 ± 127	1.8 ± 0.2	26 ± 7
Transversal	0.32 ± 0.02	0.18 ± 0.03	556 ± 102	1.7 ± 0.3	24 ± 2
Cold rolled sample					
Longitudinal	0.35 ± 0.02	0.16 ± 0.03	813 ± 323	6.3 ± 1.0	11 ± 1
Transversal	0.35 ± 0.02	0.10 ± 0.01	911 ± 336	2.7 ± 0.4	11 ± 1

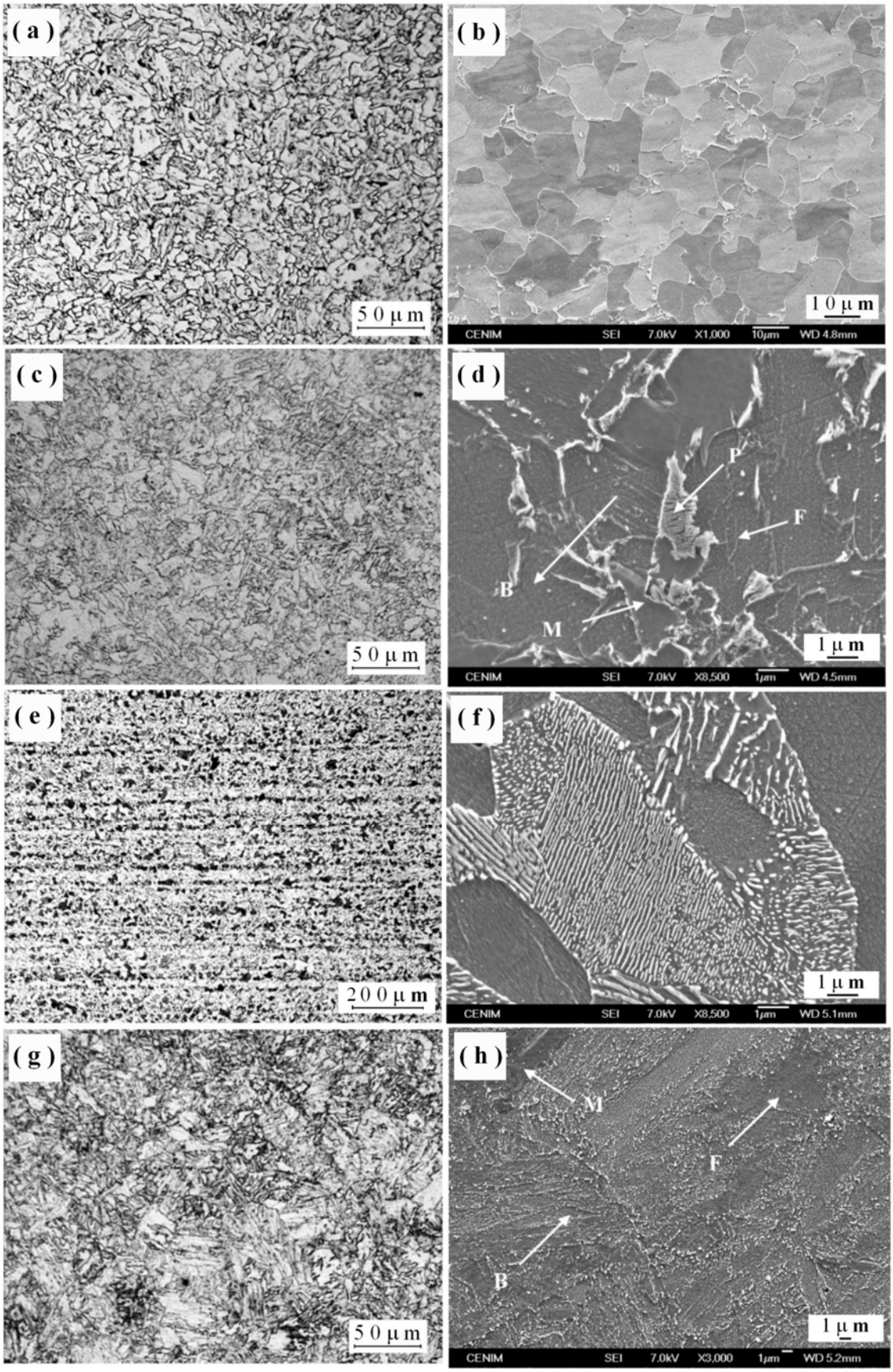

Figure 1 Light optical micrographs and scanning electron micrographs of hot rolled specimens parallel to the rolling direction: (a)(b) Sample S1: *CR*=7 ºC/s, *CT*=500 ºC; (c)(d) Sample S2: *CR*=60 ºC/s, *CT*=500 ºC; (e)(f) Sample S3: *CR*=7 ºC/s, *CT*=650 ºC; (g)(h) Sample S4: *CR*=60 ºC/s, *CT*=650 ºC. B is bainite, M is martensite, F is ferrite and P is pearlite.

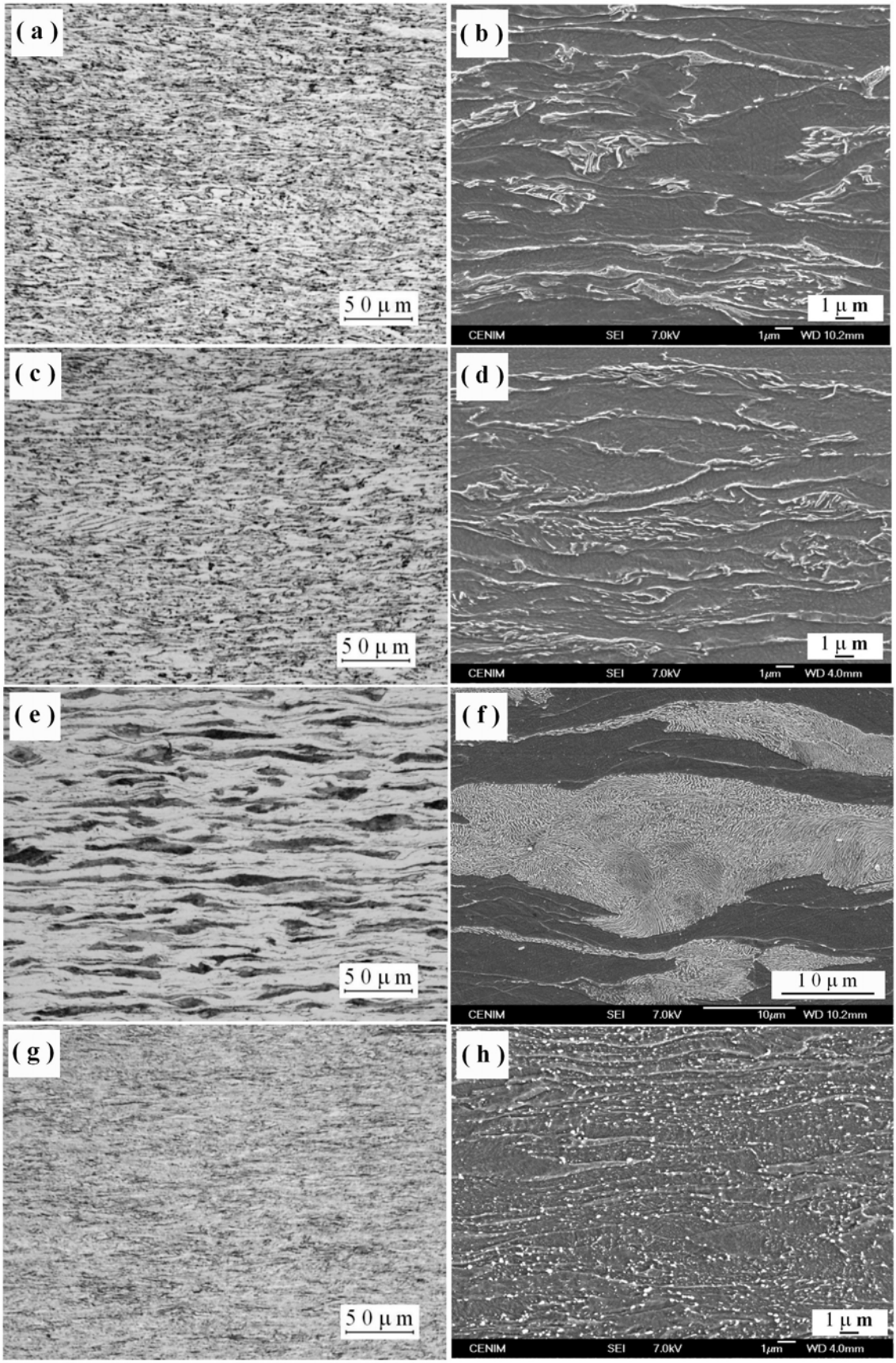

Figure 2 Light optical micrographs and scanning electron micrographs of 68% cold rolled specimens parallel to the rolling direction: (a)(b) Sample S1: *CR*=7 ºC/s, *CT*=500 ºC; (c)(d) Sample S2: *CR*=60 ºC/s, *CT*=500 ºC; (e)(f) Sample S3: *CR*=7 ºC/s, *CT*=650 ºC; and (g)(h) Sample S4: *CR*=60 ºC/s, *CT*=650 ºC.

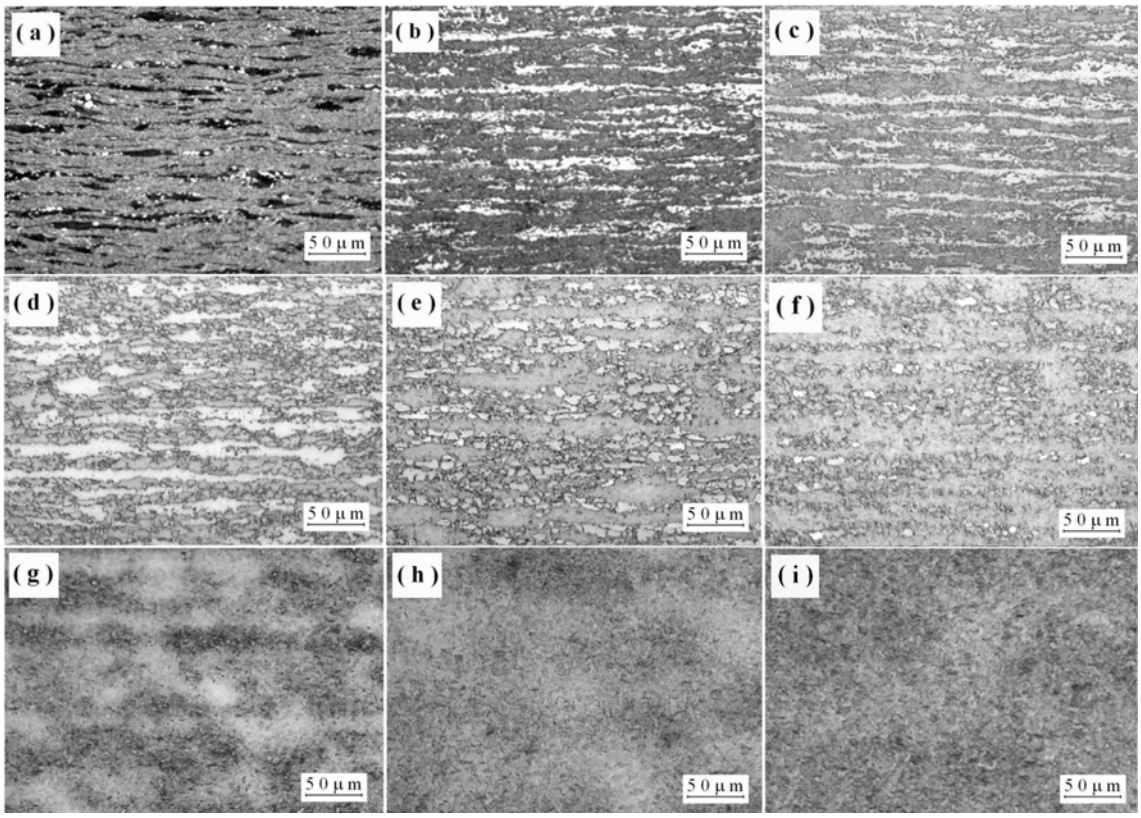

Figure 3 Optical micrographs from intercritical annealed samples: (a) at 750 ºC for 1 s; (b) at 750 ºC for 20 s; (c) at 750 ºC for 100 s; (d) at 800 ºC for 1 s; (e) at 800 ºC for 20 s; (f) at 800 ºC for 100 s; (g) at 850 ºC for 1 s; (h) at 850 ºC for 20 s; (i) at 850 ºC for 100 s. Initial microstructure: cold rolled sample S3 (*CR*=7 ºC/s, *CT*=650 ºC). LePera reagent.

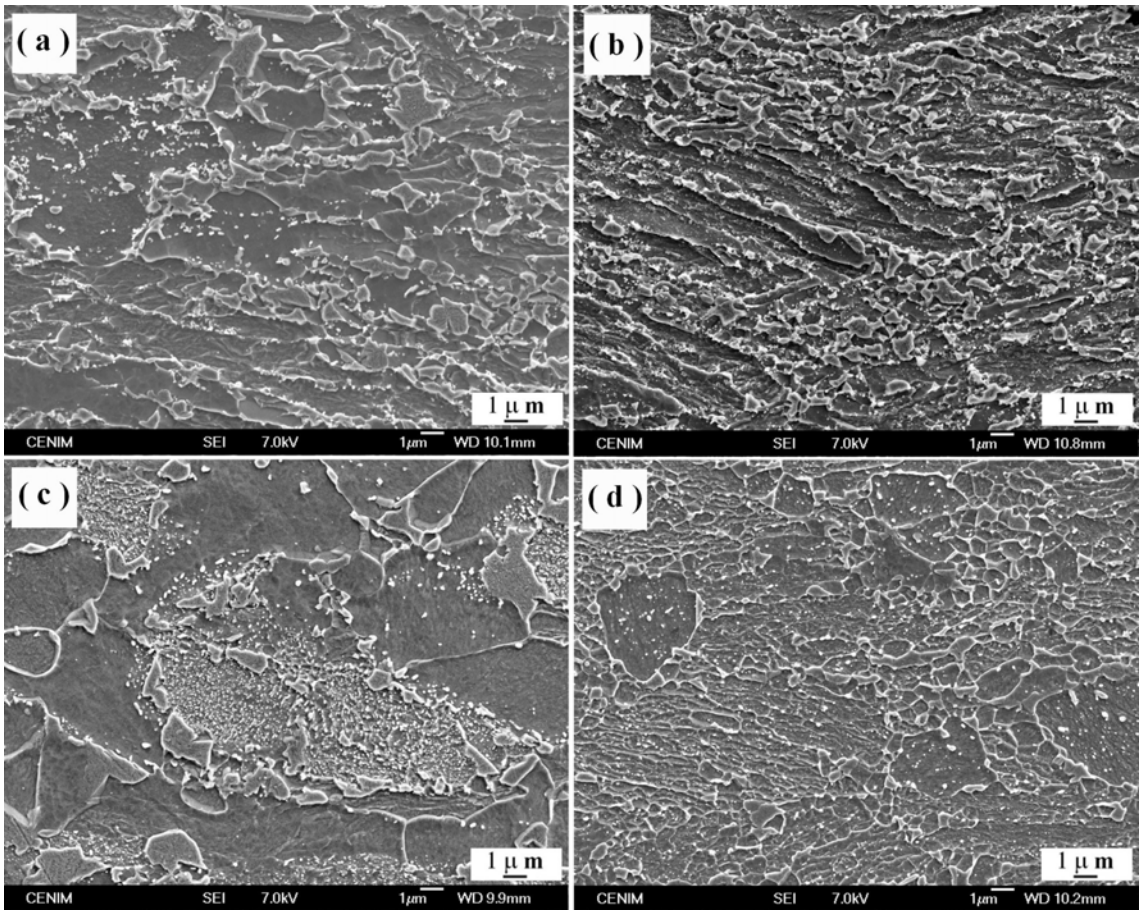

Figure 4 Scanning electron micrographs corresponding to the beginning of the austenitisation process in annealed samples at 750 ºC for 1 s. Initial microstructure: (a) sample S1 (*CR*=7 ºC/s, *CT*=500 ºC); (b) sample S2 (*CR*=60 ºC/s, *CT*=500 ºC); (c) sample S3 (*CR*=7 ºC/s, *CT*=650 ºC); and (d) sample S4 (*CR*=60 ºC/s, *CT*=650 ºC). 2 pct Nital etching solution.

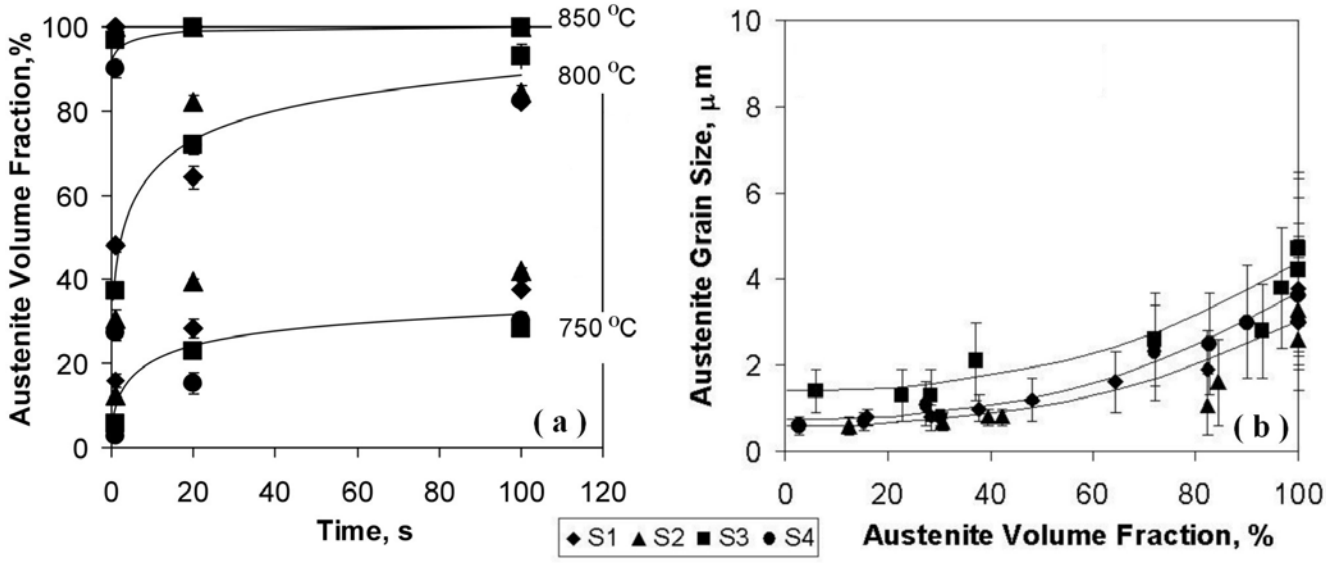

Figure 5 Evolution of (a) austenite volume fraction and (b) austenite grain size during intercritical annealing. Sample S1 (*CR*=7 ºC/s, *CT*=500 ºC); Sample S2 (*CR*=60 ºC/s, *CT*=500 ºC); Sample S3 (*CR*=7 ºC/s, *CT*=650 ºC); and Sample S4 (*CR*=60 ºC/s, *CT*=650 ºC).

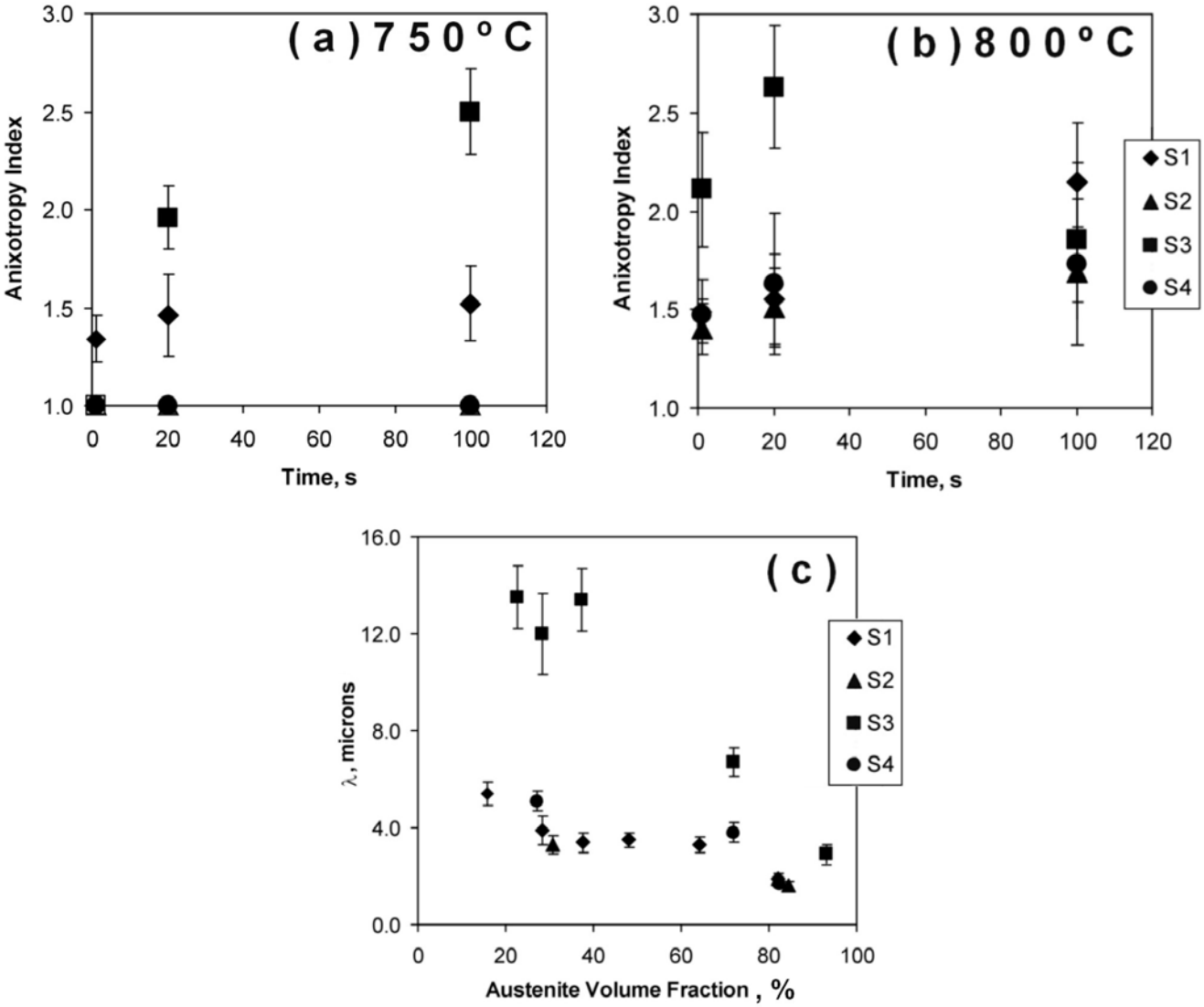

Figure 6 Evolution of microstructural banding during intercritical annealing: Anisotropy index (a) at 750 ºC and (b) at 800 ºC of soaking temperature; and (c) mean edge-to-edge spacing of the bands, λ. Sample S1 (*CR*=7 ºC/s, *CT*=500 ºC); Sample S2 (*CR*=60 ºC/s, *CT*=500 ºC); Sample S3 (*CR*=7 ºC/s, *C*T=650 ºC); and Sample S4 (*CR*=60 ºC/s, *CT*=650 ºC).

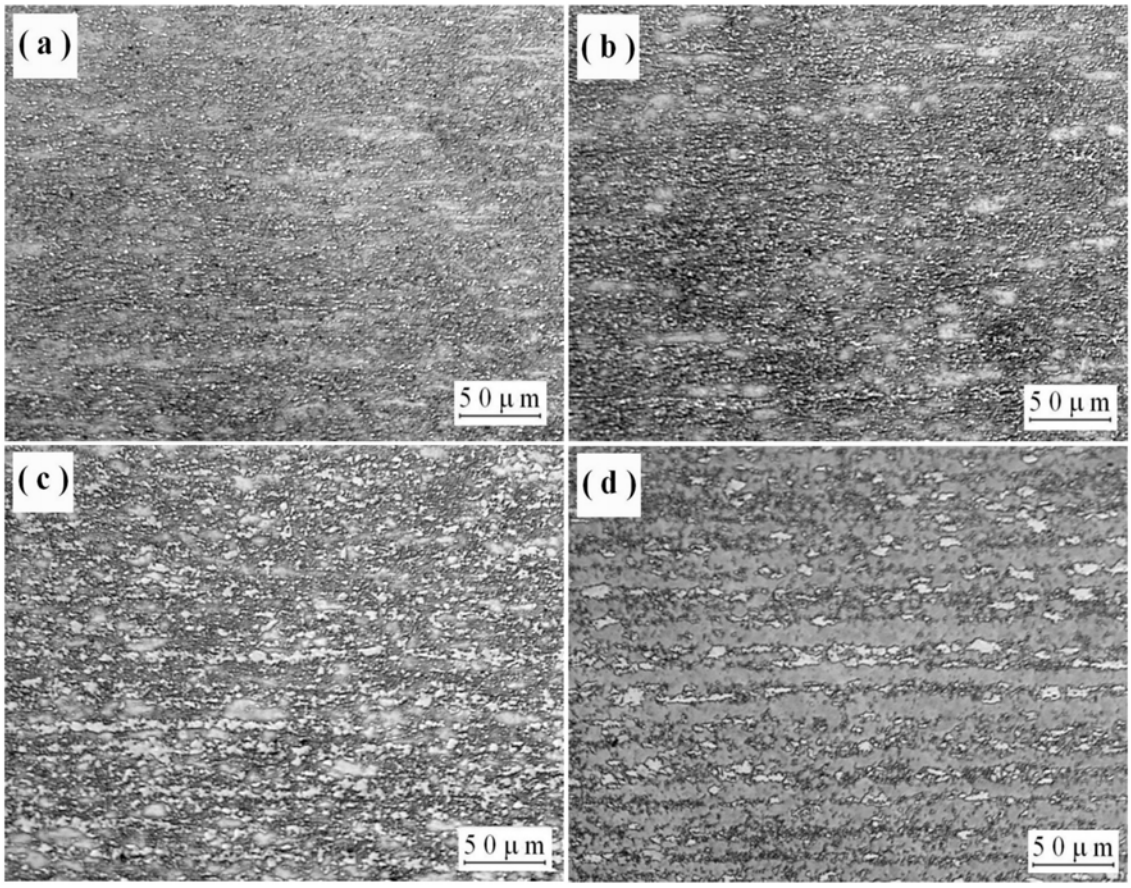

Figure 7 Evolution of microstructural banding during intercritical annealing in sample S4 (*CR*=60 ºC/s, *CT*=650 ºC): (a) 750 ºC, 20 s; (b) 750 ºC, 100 s; (c) 800 ºC, 1 s; and (d) 800 ºC, 20 s. LePera reagent.